

Supporting Information

Electrochromic properties of novel octa-pinene substituted double-decker Ln(III) (Ln = Eu, Er, Lu) phthalocyanines with distinctive near-IR absorption

Wei Zheng, Bei-Bei Wang, Jian-Cheng Lai, Cheng-Zhang Wan, Xin-Rong Lu, Cheng-Hui Li*, and Xiao-Zeng You*

Content lists:

Figure S1. MALDI-TOF mass spectra of compounds ErPc^*_2 with DHB as the matrix; isotopic patterns for the corresponding molecular ions are shown in insets.

Figure S2. MALDI-TOF mass spectra of compounds LuPc^*_2 with DHB as the matrix; isotopic patterns for the corresponding molecular ions are shown in insets.

Figure S3. A simplified molecular orbit diagram for LnPc^*_2 .

Figure S4. Electronic circular dichroism spectra for LnPc^*_2 in DCM. ($C_{\text{EuPc}^*_2} = 1.05 \times 10^{-5}$ mol/L, $C_{\text{ErPc}^*_2} = 1.46 \times 10^{-5}$ mol/L, $C_{\text{LuPc}^*_2} = 1.00 \times 10^{-5}$ mol/L)

Figure S5. SWV of LnPc^*_2 on Pt (glassy carbon) in DCM/TBAP (-0.2 ~ 2 V) and DMF/TBAP (-2.8 ~ -1 V), SWV parameters: pulse size = 100 mV; step size: 5 mV; frequency: 25 Hz. (a) EuPc^*_2 ; (a) ErPc^*_2 ; (a) LuPc^*_2 ;

Figure S6. *In-situ* UV/Vis spectral changes of ErPc^*_2 in DCM containing 1M TBAP at (a) 0.8 V; (b) -0.2 V; (c) -1.4 V. (vs. SCE)

Figure S7. *In-situ* UV/Vis spectral changes of LuPc^*_2 in DCM containing 1M TBAP at (a) 0.8 V; (b) -0.2 V; (c) -1.4 V. (vs. SCE)

Figure S8. T% changes of **ErPc^{*}₂**/ITO at two wavelenghtes versus time by repeating the potential steps using 0 V and +1.0 V with a residence time of 25 s in H₂O/LiClO₄ electrolyte system.

Figure S9. T% changes of **LuPc^{*}₂**/ITO at two wavelenghtes versus time by repeating the potential steps using 0 V and +1.0 V with a residence time of 25 s in H₂O/LiClO₄ electrolyte system.

Table S1. Maximum concentration of **LnPc^{*}₂** dissolved in different solvents .

Table S2. UV/Vis/NIR absorption data for **LnPc^{*}₂**.

Table S3. Coloration efficiency of **LnPc^{*}₂**.

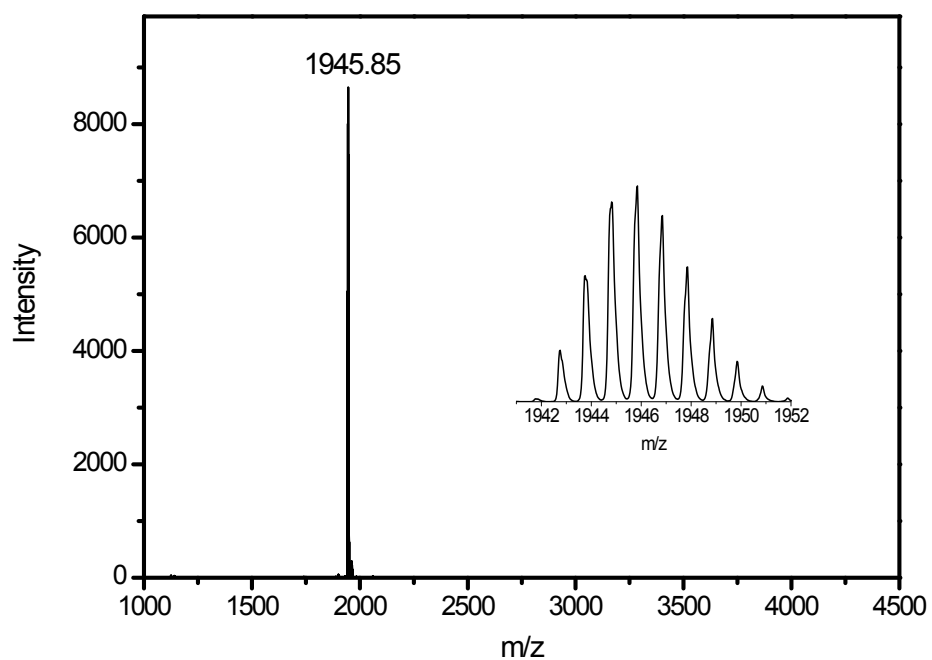


Figure S1. MALDI-TOF mass spectra of compounds **ErPc^{*}₂** with DHB as the matrix; isotopic patterns for the corresponding molecular ions are shown in insets.

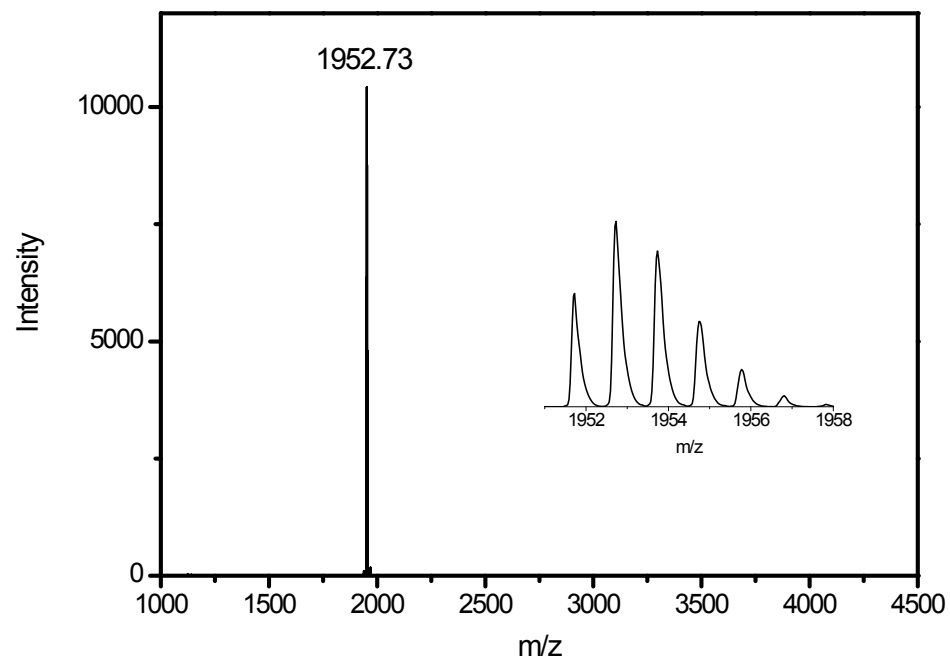


Figure S2. MALDI-TOF mass spectra of compounds **LuPc^{*}₂** with DHB as the matrix; isotopic patterns for the corresponding molecular ions are shown in insets.

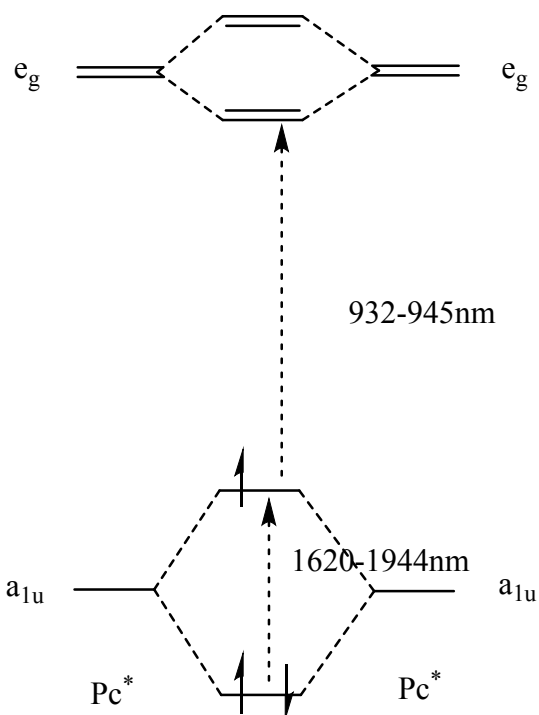


Figure S3. A simplified molecular orbit diagram for LnPc^*_2 .

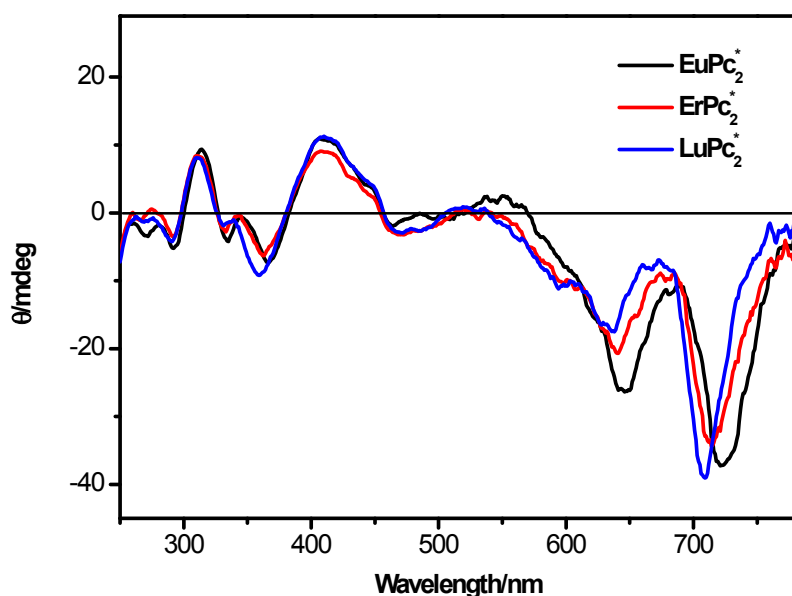


Figure S4. Electronic circular dichroism spectra for LnPc^*_2 in DCM. ($C_{\text{EuPc}^*2} = 1.05 \times 10^{-5}$ mol/L, $C_{\text{ErPc}^*2} = 1.46 \times 10^{-5}$ mol/L, $C_{\text{LuPc}^*2} = 1.00 \times 10^{-5}$ mol/L)

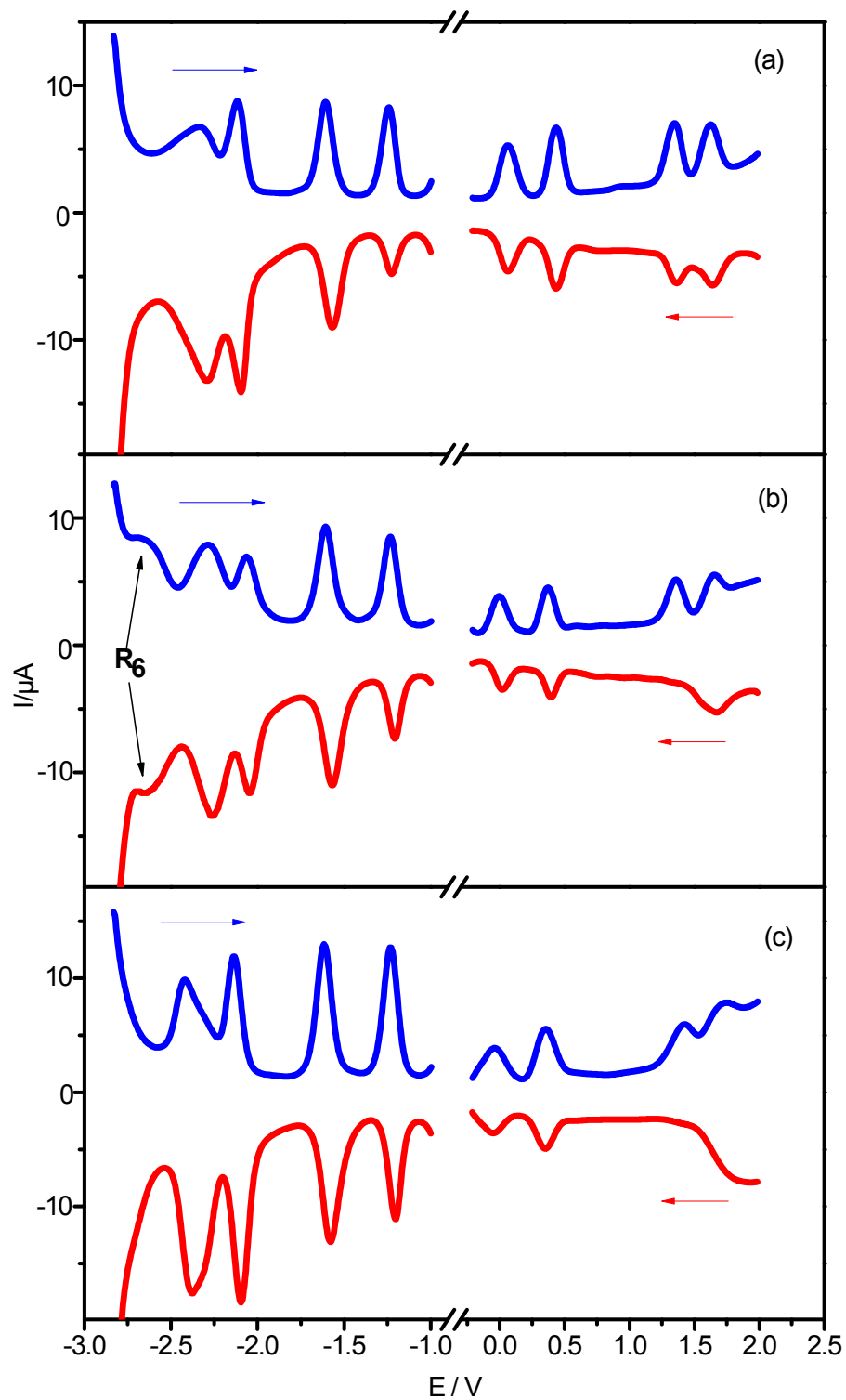
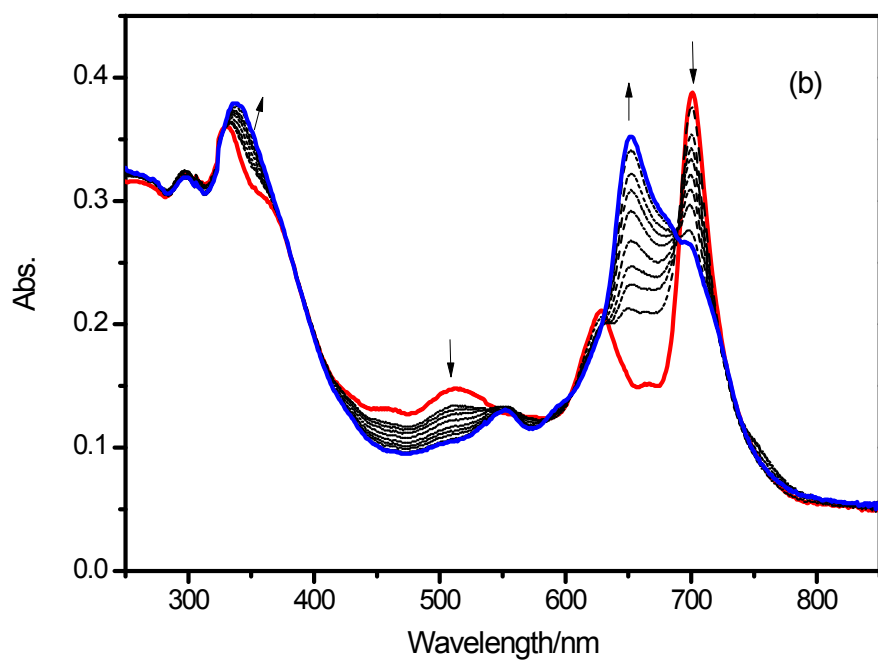
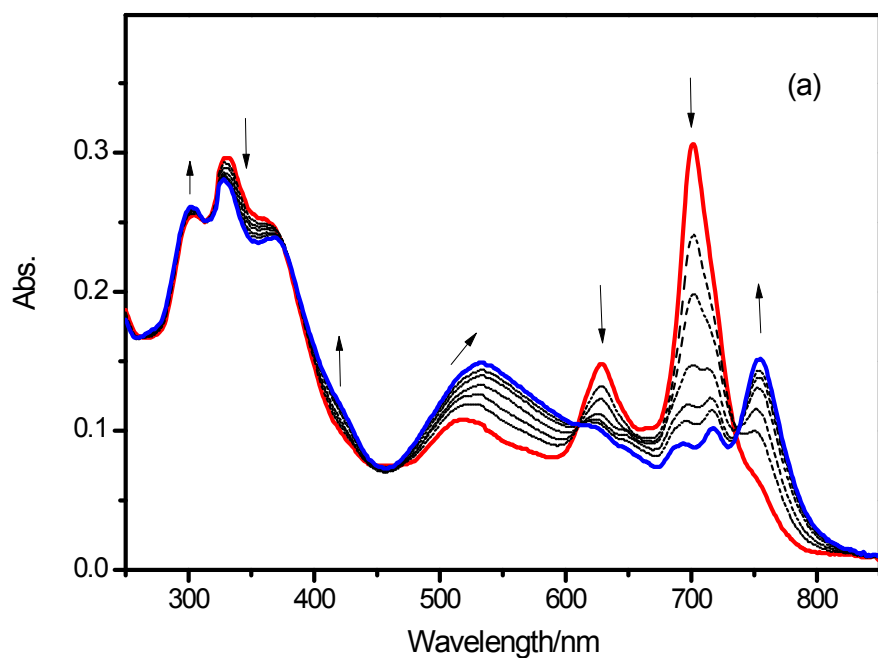


Figure S5. SWV of **LnPc*₂** on Pt (glassy carbon) in DCM/TBAP (-0.2 ~ 2 V) and DMF/TBAP (-2.8 ~ -1 V), SWV parameters: pulse size = 100 mV; step size: 5 mV; frequency: 25 Hz. (a) **EuPc*₂**; (a) **ErPc*₂**; (a) **LuPc*₂**;



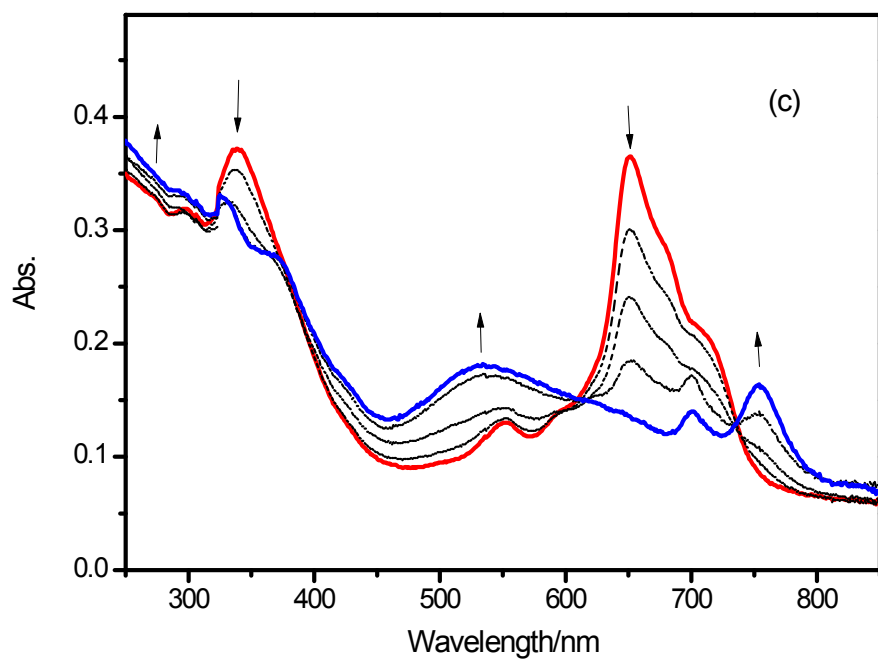
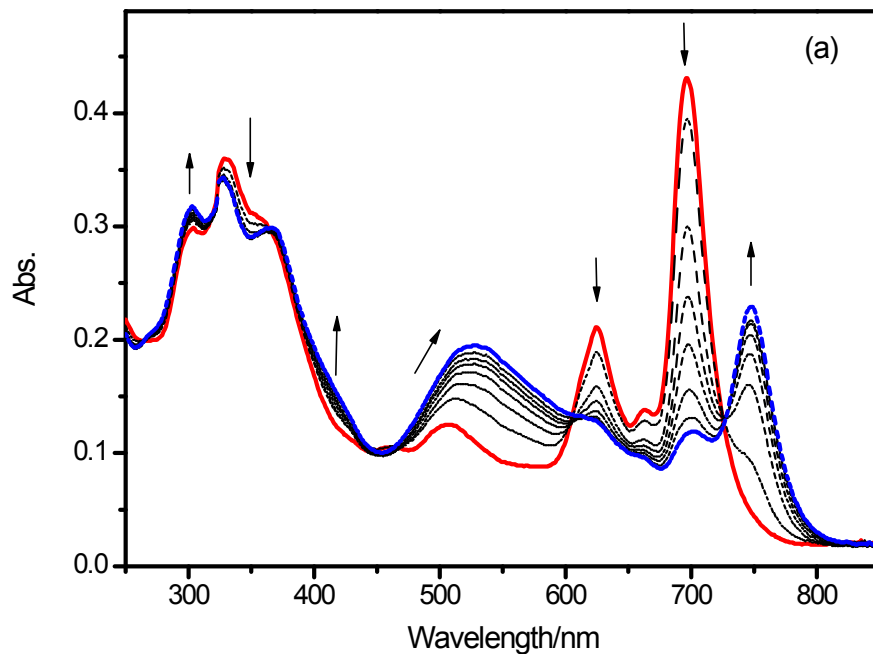


Figure S6. *In-situ* UV/Vis spectral changes of ErPc^*_2 in DCM containing 1M TBAP at (a) 0.8 V; (b) -0.2 V; (c) -1.4 V. (vs. SCE)



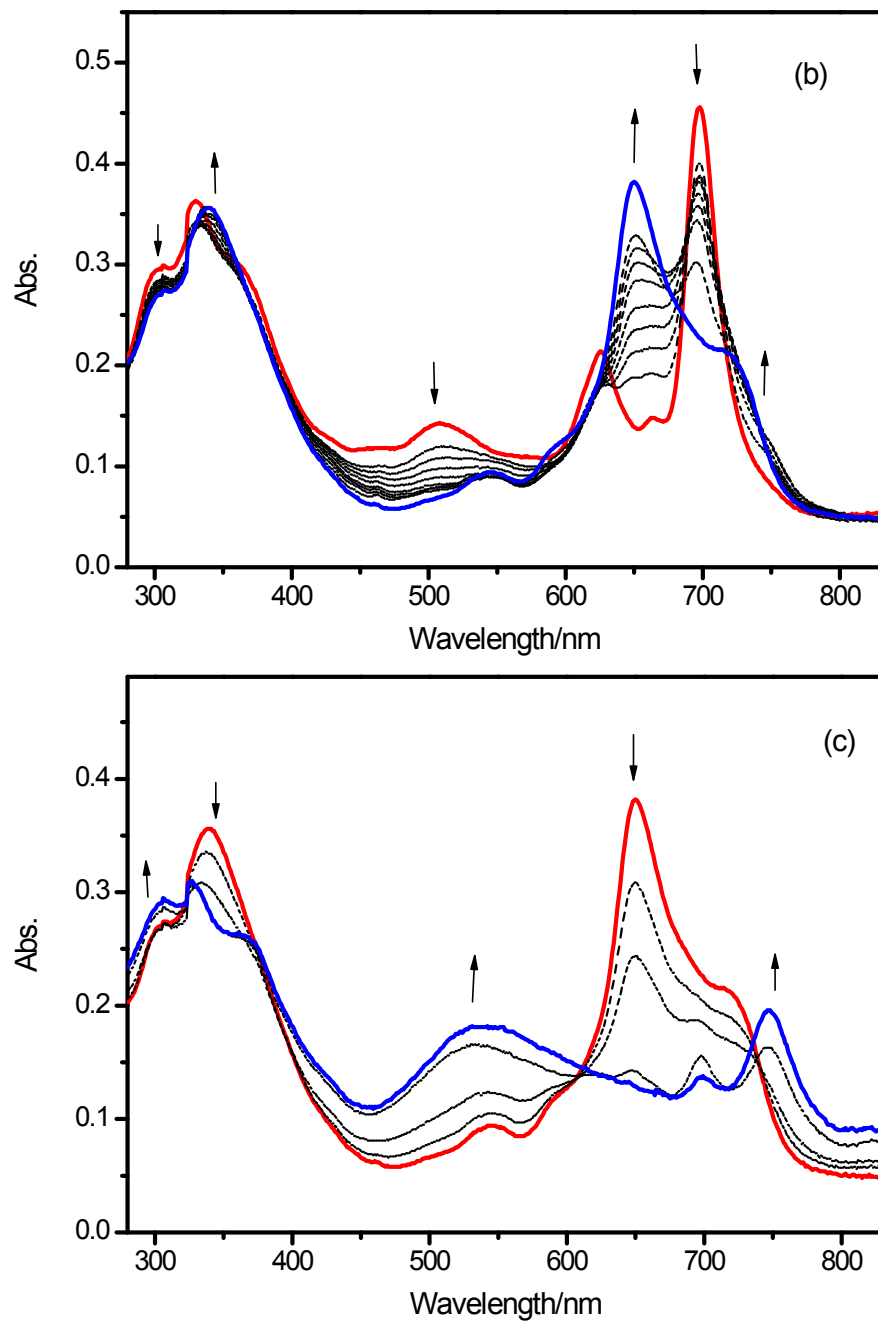


Figure S7. *In-situ* UV/Vis spectral changes of **LuPc^{*}₂** in DCM containing 1M TBAP at (a) 0.8 V; (b) -0.2 V; (c) -1.4 V. (vs. SCE)

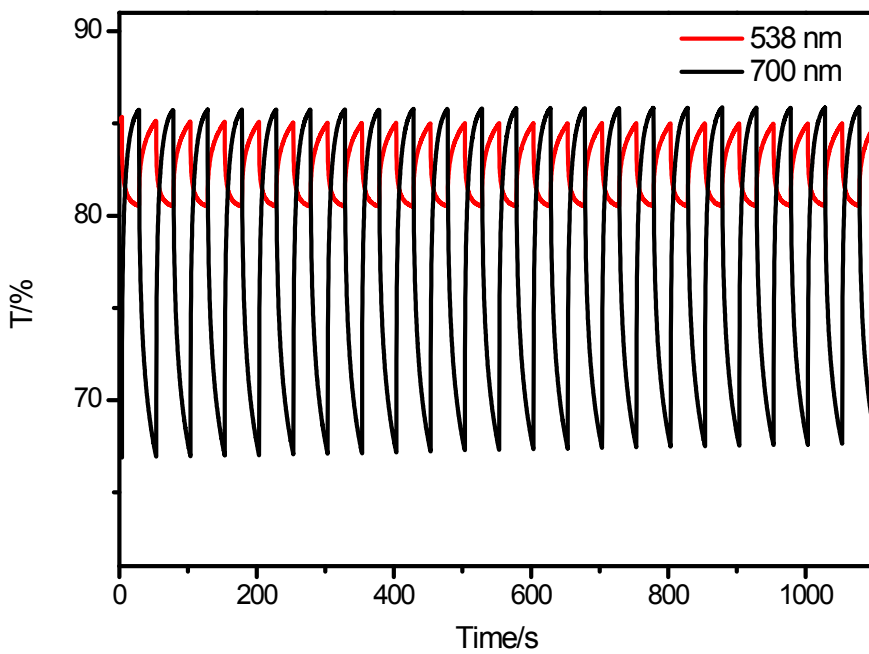


Figure S8. T% changes of $\text{ErPc}^*_2/\text{ITO}$ at two wavelenghtes versus time by repeating the potential steps using 0 V and +1.0 V with a residence time of 25 s in $\text{H}_2\text{O}/\text{LiClO}_4$ electrolyte system.

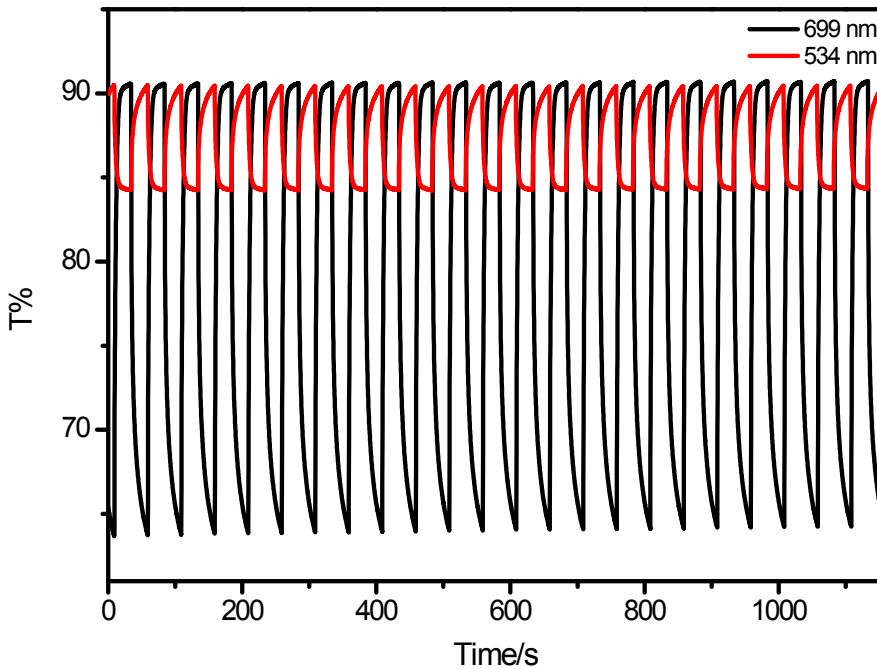


Figure S9. T% changes of $\text{LuPc}^*_2/\text{ITO}$ at two wavelenghtes versus time by repeating the potential steps using 0 V and +1.0 V with a residence time of 25 s in $\text{H}_2\text{O}/\text{LiClO}_4$ electrolyte system.

Table S1. Maximum concentration of **LnPc*₂** dissolved in different solvent .

Solvent	Polarity	Solubility (mol/L)		
		EuPc*₂	ErPc*₂	LuPc*₂
n-pentane	0	0.38	0.36	0.40
Ethyl ether	2.9	0.10	0.15	0.13
Methylene dichloride	3.4	0.12	0.18	0.20
Tetrahydrofuran	4.2	0.20	0.23	0.25
Ethyl acetate	4.3	0.09	0.08	0.08
Chloroform	4.4	0.24	0.29	0.30
Acetone	5.4	0.10	0.08	0.12
Acetonitrile	6.2	5×10 ⁻⁴ -	5×10 ⁻⁴	4×10 ⁻⁴
Dimethyl formamide	6.4	2.5×10 ⁻²	1.2×10 ⁻²	1.6×10 ⁻²
Methanol	6.6	1.5×10 ⁻³	1.3×10 ⁻³	2.2×10 ⁻³
Dimethyl sulfoxide	7.2	1.6×10 ⁻³	2.5×10 ⁻³	1.8×10 ⁻³
Water	10.2	-	-	-

Table S2. UV/Vis/NIR absorption data for **LnPc*₂**.

	$\lambda[\text{nm}] (\epsilon[10^4 \text{ L} \cdot \text{cm}^{-1} \cdot \text{mol}^{-1}])$						
	N	B (soret)	Blue valence	Q_{vib}	Q	Red valence ^[a]	Inter valence ^[a]
EuPc* ₂	300 (6.596)	332(9.058)	525 (2.289)	633 (5.048)	709 (9.616)	932 (0.221)	1944 (0.952)
ErPc* ₂	302 (4.447)	330 (5.496)	516 (4.027)	627 (2.531)	699 (6.992)	938 (0.203)	1693 (0.531)
LuPc* ₂	304 (5.654)	329 (7.044)	504 (1.751)	623 (3.048)	696 (10.298)	945 (0.330)	1620 (0.844)

[a] measured in CCl₄.**Table S3.** Coloration efficiency of **LnPc*₂**.

λ	E (V)	CE / $\text{cm}^2 \cdot \text{C}^{-1}$
538 nm (EuPc* ₂)	0.0 +1.0	196.56 204.48
538 nm (ErPc* ₂)	0.0 +1.0	224.00 229.83
534 nm (LuPc* ₂)	0.0 +1.0	284.06 145.41
708 nm (EuPc* ₂)	0.0 +1.0	823.63 841.51
700 nm (ErPc* ₂)	0.0 +1.0	963.62 956.84
699 nm (LuPc* ₂)	0.0 +1.0	1356.01 830.45